Металлофиз. новейшие технол. / Metallofiz. Noveishie Tekhnol.
2015, т. 37, № 4, сс. 455–473
Оттиски доступны непосредственно от издателя
Фотокопирование разрешено только
в соответствии с лицензией

PACS numbers: 61.72.Bb, 61.72.sd, 64.70.kd, 64.75.Bc, 65.40.G-, 82.60.Lf, 88.30.rd

The Statistical-Thermodynamic Theory of $P-c-T$-Dependences for Zirconium–Nickel Alloy Trihydride $ZrNiH_3$

S. Yu. Zaginaichenko, Z. A. Matysina*, D. V. Schur, D. A. Zaritskii*, and M. A. Polischuk

I. M. Frantsevich Institute for Problems of Materials Science, N. A. S. of Ukraine,
3 Krzhizhanovsky Str.,
03142 Kyiv, Ukraine
**Oles Honchar Dnipropetrovsk National University,*
13 Naukova Str.,
49050 Dnipropetrovsk, Ukraine

The theory of hydrogen solubility in Zr–Ni metallide of equiatomic composition is developed on the basis of molecular-kinetic concepts. The functional dependences of hydrogen content in the crystal on temperature and pressure are determined. As stipulated, the hydrogen sorption processes are realized at the sufficiently low pressures (of about 1 atm) and the moderate temperatures (of the room-temperature order). The isotherms and isopleths of hydrogen solubility are calculated. The possibility of manifestation of the hysteresis effect is ascertained. As shown, the dependence of natural logarithm of pressure on the inverse temperature for the studied alloy is a strictly linear. The results of theoretical calculations are compared with a lot of experimental data.

На підґрунті молекулярно-кінетичних уявлень розроблено теорію розчинности водню в металіді Zr–Ni еквіатомового складу. Визначено функціональну залежність вмісту Гідроґену в кристалі від температури та тиску. Обумовлено, що процеси сорбції водню реалізуються при досить малих тисках (порядку 1 атм.) та низьких температурах (порядку кімнатної). Розраховано ізотерми та ізоплети розчинности водню. Встановлено можливість прояву гістерезного ефекту. Показано, що залежність натурального логарифму тиску від оберненої температури для досліджуваного стопу є строго лінійною. Результати теоретичних розрахунків зіставлено з численними експериментальними даними.

На основе молекулярно-кинетических представлений разработана теория растворимости водорода в металлиде Zr–Ni эквиатомного состава. Определена функциональная зависимость содержания водорода в кристалле от температуры и давления. Обусловлено, что процессы сорбции водорода реализуются при достаточно малых давлениях (порядка 1 атм.) и низких

температурах (порядка комнатной). Рассчитаны изотермы и изоплеты растворимости водорода. Установлена возможность проявления гистерезисного эффекта. Показано, что зависимость натурального логарифма давления от обратной температуры для исследуемого сплава является строго линейной. Результаты теоретических расчётов сопоставлены с многочисленными экспериментальными данными.

Key words: statistical theory, hydrogenation, hydrogen solubility, hysteresis effect, Zr–Ni metallide, $ZrNiH_3$ crystal.

(Received 5 December, 2014)

1. INTRODUCTION

Promising area of science—atomic-hydrogen energetics continues to develop. Investigations of metallides, including zirconium-nickel alloy [1–20], with high hydrogen sorption properties have attracted the attention of scientists in search of reliable efficient chemical hydrogen accumulator, as ecology-clean energy storage.

Metallides have unique physical and chemical properties such as superconductivity and ferromagnetism; they are used as reinforcing material, biological implants, *etc*.

Zirconium–nickel alloy of equiatomic composition, which is the material of a new generation, refers to as the promising hydrogen sorbent and not yields to the compound $LaNi_5$ in its hydrogen sorption properties. Thus, hydrogen content in $ZrNiH_3$ hydride reaches $\cong 1.96\%$ wt. [21, 22].

Metallides and their hydrides are prepared using the methods of powder metallurgy by sintering a mixture of powders [21–29]. The zirconium–nickel alloys are formed in sufficiently mild conditions: at room temperature and atmospheric pressure. Furthermore, a radiation-thermal synthesis in the regime of thermal explosion with bombardment of samples by accelerator is used, as well as a 'cold fusion' when, after preliminary irradiation of the samples, hydrides synthesis is realized by slow cooling in a hydrogen atmosphere (1 atm) from 300–350°C to room temperature. In recent years, high temperature synthesis in regime, realized at the exothermic reaction condition of combustion of the powder at about 1500°C in a hydrogen atmosphere, is also developed.

In the $ZrNi + H_2$ system, the hydride phases (first ZrNiH, and then $ZrNiH_3$) are formed according to chemical reactions:

$$ZrNi + \frac{x}{2} H_2 \rightarrow ZrNiH + \frac{x-1}{2} H_2 \rightarrow ZrNiH_x,\ x \cong 3, \qquad (1)$$

i.e. about three hydrogen atoms are absorbed per formula unit of metal-

lide ZrNi.

The development of statistical theory of hydrogen saturation of ZrNi alloy is interesting for establishment of the optimal conditions of the accumulation and storage of hydrogen in this and similar systems.

To solve this problem, the free energy is calculated, its dependences on temperature, pressure, hydrogen concentration, and energy parameters of the interatomic interactions is ascertained. The calculations are performed using simplifying assumptions: the crystal lattice is supposed geometrically perfect, only pairwise interaction of neighbouring atoms is taken into account, an arrangement of hydrogen atoms is considered only for interstices of the two types, tetrahedral and bipyramidal, and the weak interaction between hydrogen atoms is neglected (see [30, 31]).

2. STRUCTURE AND EXPERIMENTAL STUDIES OF $ZrNiH_3$ GIDROMETALLIDE

The structure of ZrNi crystal consists of identical fragments—trigonal biprisms, which are coupled together along the bases, perpendicular to the lattice parameter $\bar{a}$ (x-axis) and along lateral faces in planar planes, perpendicular to the parameter $\bar{b}$ (z-axis) (Fig. 1). They form

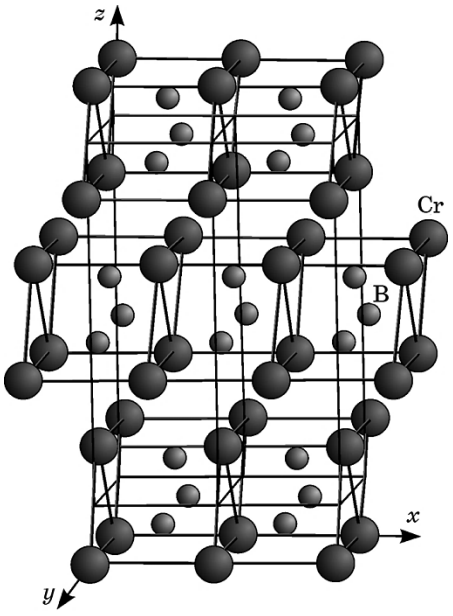

Fig. 1. The crystal lattice of the CrB type. The parallel-displaced layers are shown with formation of zigzag chains along the z-axis by the chromium and boron atoms [61].

parallel layers in the planes (x, y), which are shifted relative to each other in these planes. Because of this shift, as easily seen from Fig. 1, nickel and zirconium atoms form a zigzag chain along z-axis.

Crystal of ZrNi has the D_{2h}^{17} structure of the CrB type, in which the atoms of zirconium and nickel have well-ordered arrangement with the formation of coordination polyhedrons, in which the hydrogen atoms are placed during hydrogenation (Fig. 2). The structure with the calculation of lattice parameters has been studied in numerous works [32–60]. At hydrogenation processes the hydride $ZrNiH_x$ ($x \cong 3$) is formed. The absorption maximum of the hydrogen atoms occurs for the equiatomic alloy composition Zr–Ni. The hydrogen atoms can occupy three types of interstices: distorted tetrahedron with [Zr_3Ni] faceting, trigonal bipyramid with [Zr_3Ni_2] faceting and distorted octahedron with [Zr_4Ni_2] faceting [59]. Primarily two first polyhedrons are filled (up to $x \leq 3$), and when $x > 3$ the octahedral voids begin to fill, *i.e.*, in the distribution of hydrogen atoms on their positions some ordering is observed. In all of the interstitial positions, hydrogen atoms are mainly surrounded by hydride-forming atoms of zirconium and in less by nickel atoms, which do not form hydride. Therefore, in Zr–Ni alloys

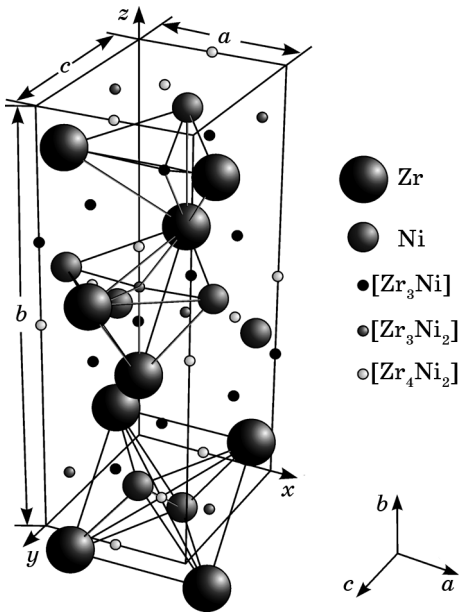

Fig. 2. The structure of crystal $ZrNiH_x$ ($x \leq 3$) of the CrB type [62]. The coordination polyhedron (distorted tetrahedron, trigonal bipyramid and octahedron) are shown with hydrogen atoms in the centre and with zirconium and nickel atoms in the vertices. The surroundings of hydrogen atoms by the nearest Zr and Ni atoms are indicated (a, b, c—lattice parameters).

TABLE. Parameters of crystal lattice (in Å) of ZrNi metallide and its hydrides of the D_{2h}^{17} structure of the CrB type.

ZrNi			ZrNiH			$ZrNiH_3$			References
a	*b*	*c*	*a*	*b*	*c*	*a*	*b*	*c*	
3.264	10.476	4.3015				3.53	10.48	4.30	[32, 33]
3.268	9.937	4.101							[34, 51, 55]
3.258	9.947	4.091				3.53	10.48	4.30	[26]
3.272	9.965	4.115	3.28	10.12	4.05	3.530	10.313	4.063	[40]
3.258	9.941	4.034				3.53	10.48	4.30	[36, 41]
3.25	9.94	4.034	3.33	10.183	4.034	3.528	10.464	4.286	[47]
3.28	10.042	4.039				3.536	10.43	4.287	[22, 29]
3.290	9.998	4.080				3.530	10.620	4.328	[43]
3.2712	9.9310	4.1072				3.530	10.48	4.30	[52]
			3.367	10.313	4.063	3.53	10.48	4.30	[54, 57]

with variable composition the concentration of the absorbed hydrogen increases with increasing of zirconium content [7].

As the result of the hydrogenation, the crystal structure is maintained the same CrB type, there is only a lattice expansion, *i.e.*, as can be seen from the Table, lattice parameters are increased.

The reducing of the temperature and pressure activates the process of absorption, and the hydrogen concentration in the crystal is increased (Fig. 3) [27], which are indicated the endothermic nature of the absorption process. The heating of the sample at temperature of $\cong 300$°C initiates a desorption process.

Figure 4 shows the graphic data of the differential thermal analysis (DTA), differential scanning calorimetry (DSC) and temperature gravimetry (TG) [61–66]. According to the paper [65], the reducing of the heat flow (endothermic peak at 264°C) during hydrogenation is caused by phase transition in a system of hydrogen atoms because of their distribution (ordering) on their positions with forming in the beginning the ZrNiH phase and then the $ZrNiH_3$ one. The increasing of the heat flow (exothermic peak at 278°C) is caused by degassing of the sample. As demonstrated by Fig. 4, *a*, the sorption processes take place at room temperatures.

Desorption of hydrogen from $ZrNiH_3$ is accompanied by the release of energy (exothermic peak on DSC graph in Fig. 4, *b* and *c*), and absorption reduces the heat flow (endothermic peak *2* in Fig. 4, *b*). Figure 4, *d* presents the decreasing of $ZrNiH_3$-hydride weight because of hydrogen release.

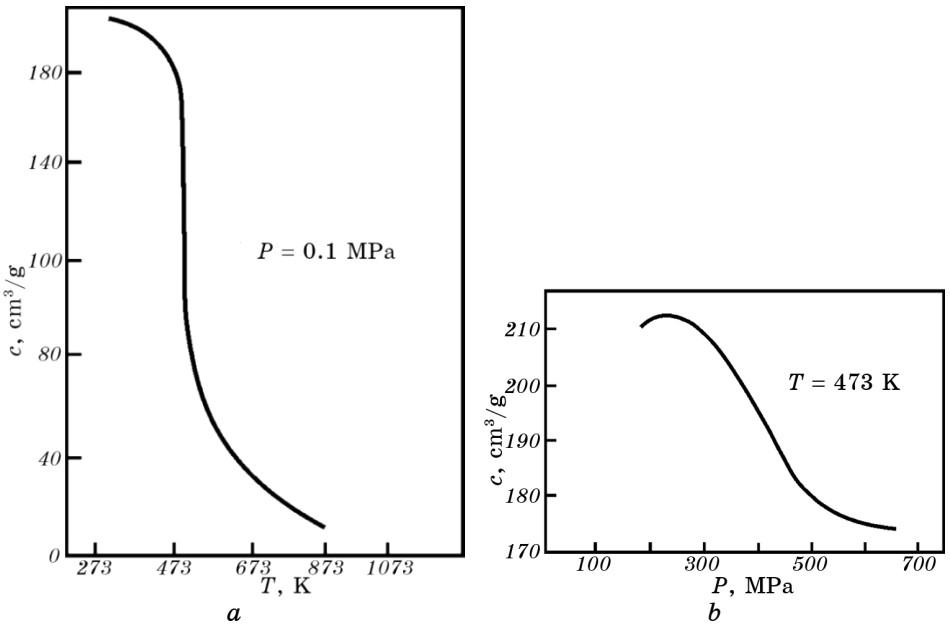

Fig. 3. Experimental dependences of hydrogen content in the ZrNi sample on temperature (*a*) and specific pressure (*b*) [27].

Figure 5 shows the sorption isotherms of hydrogen for ZrNi–H_2 systems, which were studied in works [23, 26, 36, 67–72]. The rapid increase of pressure at H/ZrNi ≅ 1 is caused by the ZrNiH-hydride formation during the absorption process. Further, there is an accumulation of hydrogen, formation of $ZrNiH_3$ phase; the isotherm has a plateau corresponding to the coexistence of two crystalline phases ZrNiH and $ZrNiH_3$ with different amounts. Then, the rapid increase of pressure during the $ZrNiH_x$ hydride ($x > 3$) formation is observed again. The authors of work [16] consider the absorption process as the realization of phase transformations with both zirconium–nickel metallide mono- and trihydride formations. As shown in Fig. 5, *a*, hysteresis effect appears in the absorption–desorption process. The hysteresis loop with increasing temperature shortens, narrows, and at sufficiently high temperatures, it should disappear. With increase of temperature, the hysteresis loop is situated ever higher along the ordinate axis. Desorption process takes place with a delay of hydrogen release; desorption curve passes below along ordinate axis at lower pressures in comparison with the absorption curve, which results in a hysteresis effect.

Figure 6 shows the sorption isopleths of ZrNi metallide in hydrogen atmosphere [68–70]. As can be seen from this figure, the dependence of logarithm of pressure on the reciprocal temperature is strictly linear. For each temperature desorption occurs at a lower pressure than

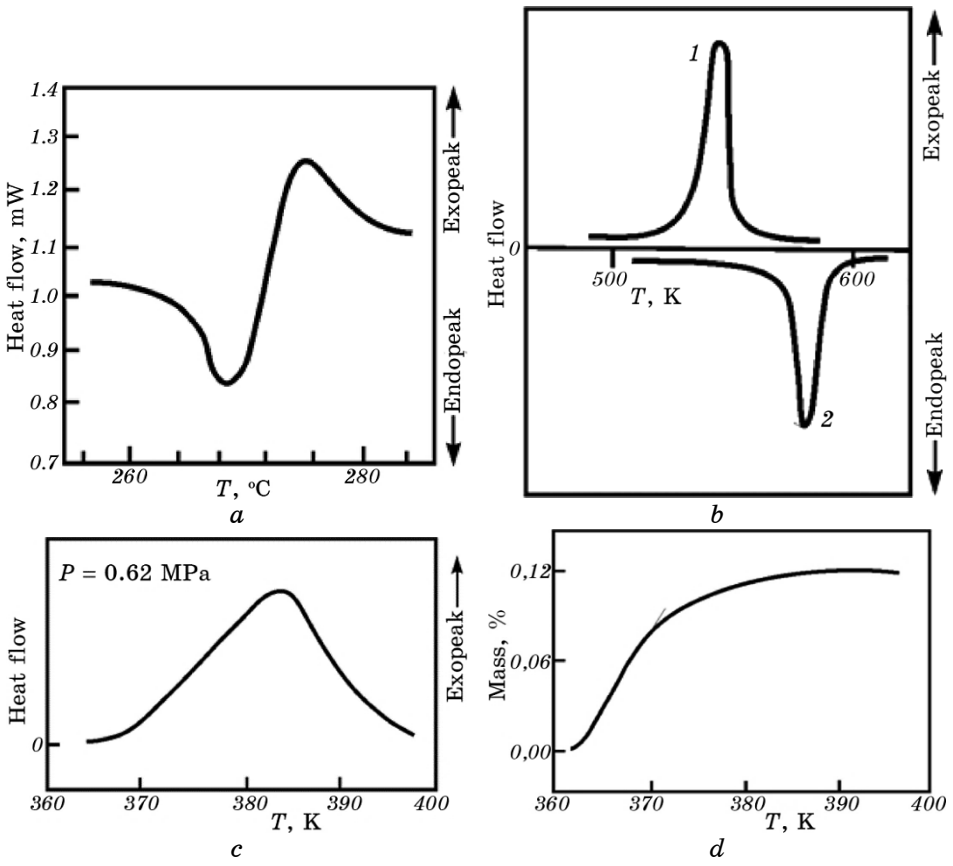

Fig. 4. Experimental plots [61–66]: DTA plot of hydrogen sorption in the $ZrNi–H_2$ system. Endopeak is at the hydrogen absorption; exopeak is at the hydrogen extraction (*a*); DSC graph—the heat flow at the dehydrogenation of $ZrNiH_3$ (peak *1*) and at the hydrogenation of ZrNi (peak *2*) as a result of heating in the regime of 5 K/min (*b*); DSC plot—the heat flow at the hydrogen yield from the $ZrNiH_3$ alloy at the heating rate of 5 K/min (*c*); TG curve—the mass loss of the $ZrNiH_3$ specimen at the hydrogen desorption (*d*).

the absorption phenomena, *i.e.*, as for the isothermal process, happens with a lag.

3. THEORY

One can calculate the free energy of $ZrNiH_3$ hydrometallide using the well-known formula [73, 74]

$$F = E - kT \ln W - kTN_{\text{H}} \ln A, \tag{2}$$

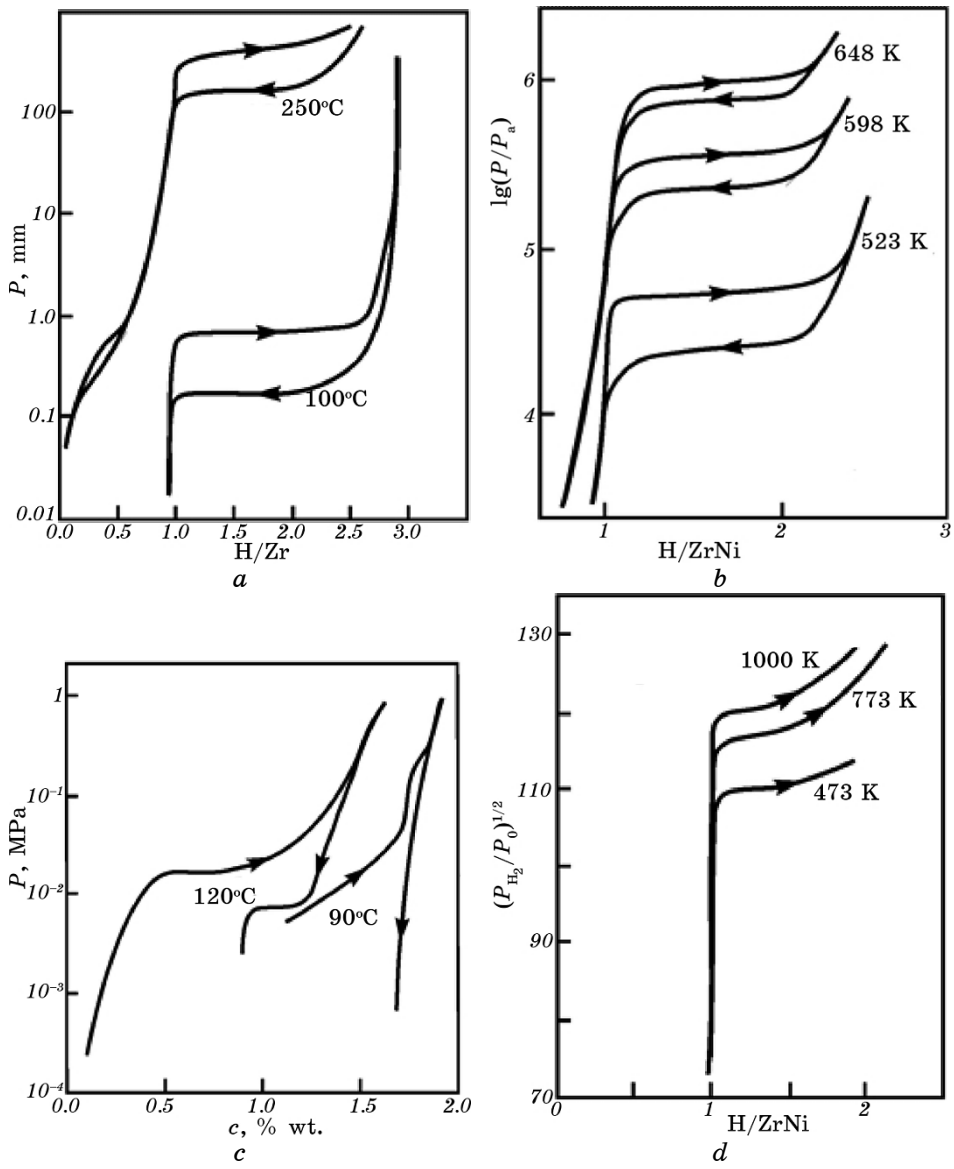

Fig. 5. Experimental isotherms of absorption–desorption for system ZrNi–H_2. The annealing temperatures are indicated [23, 26, 36, 67–72].

where E is an internal configuration energy, which determined in concerned approximation by the sum of the pair interaction energies of nickel or zirconium nearest atoms with hydrogen atoms.

In formula (2), W is a thermodynamic probability, which equals the sum of energy distinguishable states of the system, calculated accord-

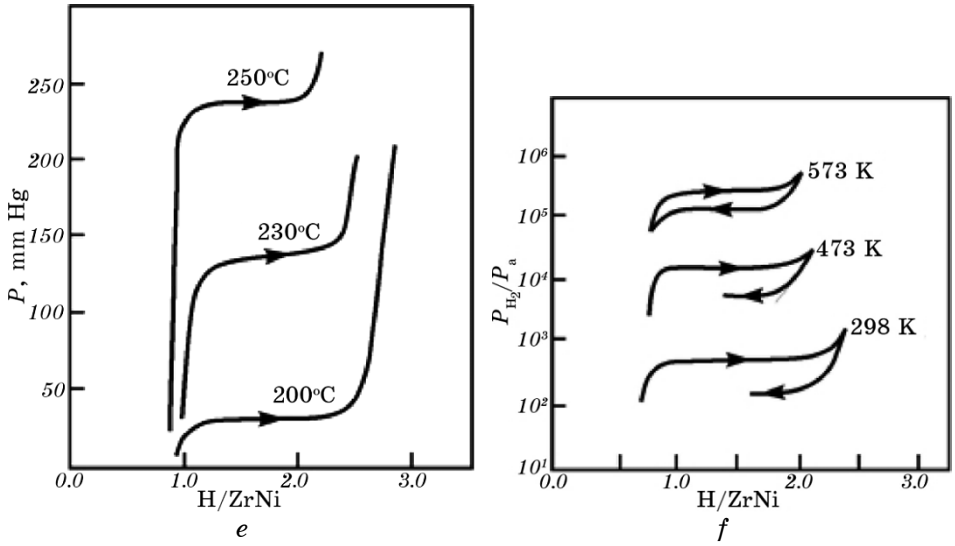

Continuation of Fig. 5.

ing to the combinatory rules, N_H is the number of hydrogen atoms in a crystal, A is their activity, k is Boltzmann constant, and T is absolute temperature. We will take into account the placement of hydrogen atoms only on tetrahedral θ interstices and bipyramidal P ones. We also introduce the next notations: N—number of zirconium atoms, the same as number of nickel atoms, $2N$ and N—number of tetrahedral and bipyramidal interstitial cites, correspondingly, N_θ and N_P—numbers of hydrogen atoms in the positions of θ and P,

$$N_H = N_\theta + N_P \tag{3}$$

is a number of hydrogen atoms in the crystal;

$$c_\theta = N_\theta/2N, \quad c_P = N_P/N, \quad c = N_H/3N, \quad c = (2c_\theta + c_P)/3 \tag{4}$$

are concentrations of hydrogen atoms in the positions θ and P, and in the crystal (in θ + P) relative to the number of interstitial cites, respectively equal $2N$, N and $3N$, wherein

$$0 \le c_\theta, c_P, c \le 1; \tag{5}$$

u_θ, u_P are the energies of the hydrogen atoms in the θ and P interstitial cites, which are equal

$$u_\theta = 3u_{ZH} + u_{NH}, \quad u_P = 3u_{ZH} + 2u_{NH}, \tag{6}$$

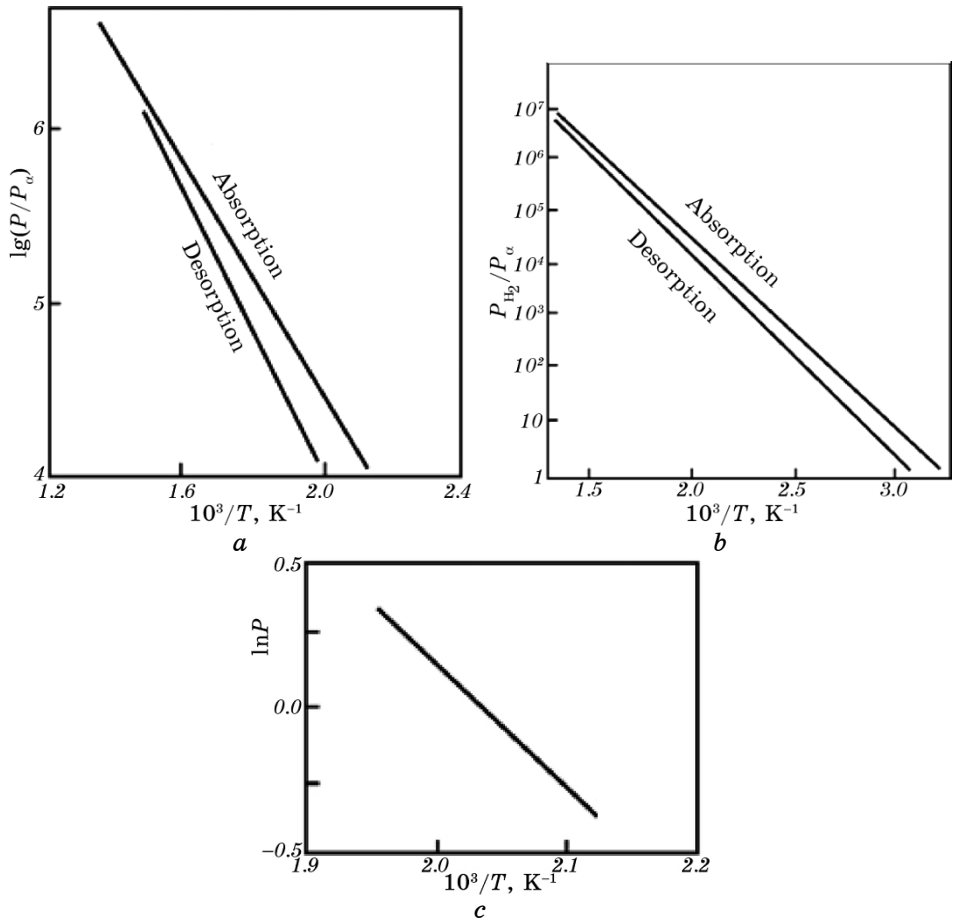

Fig. 6. Experimental isopleths for the ZrNi intermetallide in the hydrogen atmosphere (*a*), for the $ZrNiH + ZrNiH_3$ system after annealing at 1000 K (*b*), and for the ZrNi alloy in the tritium–protium atmosphere (*c*) [68–70].

u_{ZH}, u_{NH} are the interaction energies of the nearest atom pairs ZrH and NiH.

We determine the internal configuration energy by the formula

$$E = E_0 + N_\theta u_\theta + N_P u_P \tag{7}$$

and thermodynamic probability by the expression

$$W = \frac{(2N)!}{N_\theta!(2N - N_\theta)!} \frac{N!}{N_P!(N - N_P)!}. \tag{8}$$

In formula (7), the value of E_0 is determined by the terms that do not

depend on the concentration of hydrogen.

With use the Stirling's formula $\ln X! \cong X(\ln X - 1)$ valid for large values of X, one can find the natural logarithm of thermodynamic probability and then calculate the free energy taking into account Eqs. (2), (3), (7), and (8):

$$F = E_0 + N_\theta u_\theta + N_P u_P - kT\left[2N\ln 2N - N_\theta \ln N_\theta - (2N - N_\theta)\ln(2N - \right.$$
$$\left. -N_\theta) + N \ln N - N_P \ln N_P - (N - N_P)\ln(N - N_P)\right] - kT(N_\theta + N_P)\ln A. \quad (9)$$

The free energy of the system is minimal in the state of thermodynamic equilibrium. Form minimizing procedure of free energy

$$\frac{\partial F}{\partial N_\theta} = 0, \quad \frac{\partial F}{\partial N_P} = 0, \quad (10)$$

one can find equations, which determine the equilibrium content of hydrogen atoms in the θ and P interstitial cites, *i.e.*

$$\frac{u_\theta}{kT} + \ln\frac{c_\theta}{1 - c_\theta} - \ln A = 0, \quad \frac{u_P}{kT} + \ln\frac{c_P}{1 - c_P} - \ln A = 0 \quad (11)$$

or

$$c_\theta = (1 + \frac{1}{A}\exp\frac{u_\theta}{kT})^{-1}, \quad c_P = (1 + \frac{1}{A}\exp\frac{u_P}{kT})^{-1}. \quad (12)$$

At low concentrations c_θ, c_P, Eqs. (12) are simplified:

$$c_\theta = A\exp\frac{-u_\theta}{kT}, \quad c_P = A\exp\frac{-u_P}{kT}. \quad (13)$$

A hydrogen concentration versus temperature $c(T)$, according to the formulas (4) and (11) or even the simplified ones (12), at greatly differing energies u_θ, u_P may be extremal and even retrograde.

Further, we find out the possible character of the dependences $c(T)$, $c(P)$ and types of isotherms and isopleths of hydrogen solubility in metallide.

4. INTERPRETATION OF THE CALCULATIONS' RESULTS

In the case of equiprobability distribution (disordering) of the hydrogen atoms on θ and P positions, when $c \approx c_\theta \approx c_P$ (it will be at almost equal energies (6) $u \approx u_\theta \approx u_P$), taking into account the changes in lattice parameters due to an increasing of hydrogen content (see Table), which are causes of changes of the interatomic distances and dependences of energies u_θ, u_P on the hydrogen concentration c and the external pressure P,

$$u = u^0 + \alpha c + \beta P,\ \alpha = \text{const},\ \beta = \text{const}\,, \tag{14}$$

and taking into account the dependence of atomic hydrogen activity in the crystal on pressure [74],

$$A = DP^{1/2},\ D = \text{const}, \tag{15}$$

we can write one formula instead of formulas (12):

$$c = \left(1 + \frac{1}{DP^{1/2}} \exp \frac{u^0 + \alpha c + \beta P}{kT}\right)^{-1}. \tag{16}$$

This formula gives a possibility of construction the P–c–T-state diagrams of crystal and clarifies the nature of dependences $c(T)$, $c(P)$, and the forms of isotherms and isopleths of hydrogen solubility in the metallide.

Note that hydrogen saturation of metallide and external pressure of hydrogen atmosphere are competing factors: the first factor expands the crystal (reduces energy u), the second factor compresses it (increases energy u), so the coefficients α and β in Eq. (16) have opposite signs. Energy u^0 is approximately estimated using experiments (Fig. 3).

Dependence $c(T)$ is estimated by formula (16), which can be conveniently rewritten as

$$kT = \frac{u^0 + \alpha c + \beta P}{\ln\left[DP^{1/2}\,\dfrac{(1-c)}{c}\right]}. \tag{17}$$

Specifying various concentrations c at certain values of the pressure P and constants u^0, D, α, β in this formula, we can find the temperature and plot the function $c = c(T)$.

Dependence $c(P)$ can be conveniently determined by formula (16). Specifying various values of pressure P for certain values of temperature and constants u^0, D, α, β in this formula, we can count concentration c, and then plot the function $c = c(P)$.

As an example, Figs. 7, *a* and *b* show graphs of the hydrogen-content dependence for $ZrNiH_x$ hydrometallide on temperature and pressure. We are interested in these graphs in high concentrations area close to $x \cong 3$ ($c \cong x/3$). As seen from Fig. 7, at high concentrations c with a decrease in both temperature and pressure, the solubility of hydrogen in the crystal increases. At low concentrations of hydrogen, as seen from Fig. 7, *b*, character of dependences $c(T)$ and $c(P)$ changes substantially. This may be caused by the fact that at high pressures (greater than 0.3 MPa) hydrogen atoms may be pushed out of the crystal and the hydrogen content can decrease with temperature decreasing. Comparison

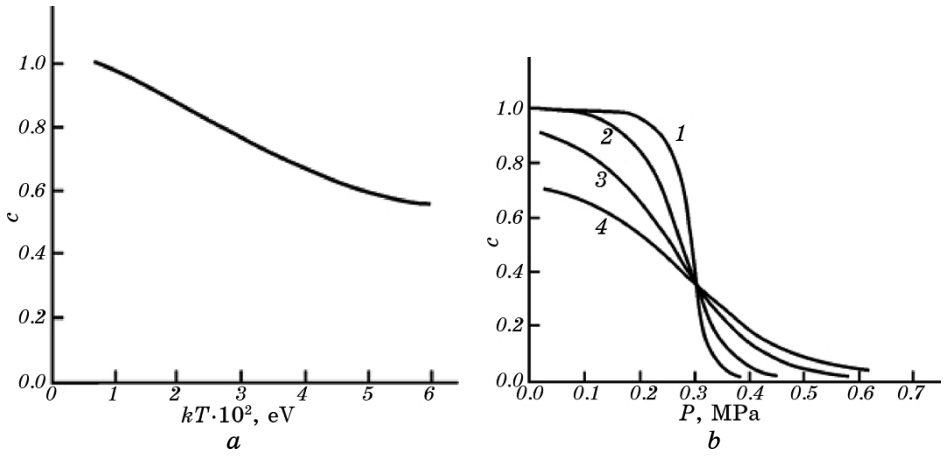

Fig. 7. The dependences of the hydrogen concentration in the $ZrNiH_x$ crystal on temperature (*a*) and pressure (*b*) calculated with use of Eqs. (16), (17) for $u^0 = 0.37$ eV, $P = 0.1$ MPa, $D = 1$ MPa$^{-1/2}$, $\alpha = 0.11$ eV, $\beta = 0$ (*a*); $u^0 = -0.17$ eV, $kT = 0.01$, 0.02, 0.04, 0.06 eV (curves *1*, *2*, *3*, *4*), $D = 1$ MPa$^{-1/2}$, $\alpha = 0$, $\beta = 0.57$ eV·MPa^{-1}.

of the calculated (see Fig. 7) and experimental (Fig. 3) dependences shows their qualitative agreement.

To construct the hydrogen solubility isotherms (dependence of ln$P$ on the concentration c) in ZrNi metallide, Eq. (16) can be rewritten in the form as follows:

$$\ln P = 2 \ln \frac{c}{A(1-c)} + \frac{2(u^0 + \alpha c + \beta P)}{kT}. \qquad (18)$$

The analysis of this formula for an extremum, when $\partial(\ln P) / \partial c = 0$, gives two values of the hydrogen-concentration extremum manifestations (maximum and minimum), which are determined (at $A = 1$ and $\beta = 0$) by the formula

$$c_{1,2} = \frac{1}{2} \pm \sqrt{\frac{1}{4} + \frac{kT}{2\alpha}}. \qquad (19)$$

It is follows from this formula that for $\alpha < 0$ with temperature increasing difference $\Delta c = c_2 - c_1$ will decrease and at $T \to \infty$ will be $c_1 = c_2$. For example, for $\alpha = -0.14$ eV and

$$\begin{aligned} &\text{at } kT = 0.020, \text{ we have } c_1 = 0.24,\ c_2 = 0.76, \\ &\text{at } kT = 0.0235, \text{ we have } c_1 = 0.31,\ c_2 = 0.69, \\ &\text{at } kT = 0.027, \text{ we have } c_1 = 0.43,\ c_2 = 0.57. \end{aligned} \qquad (20)$$

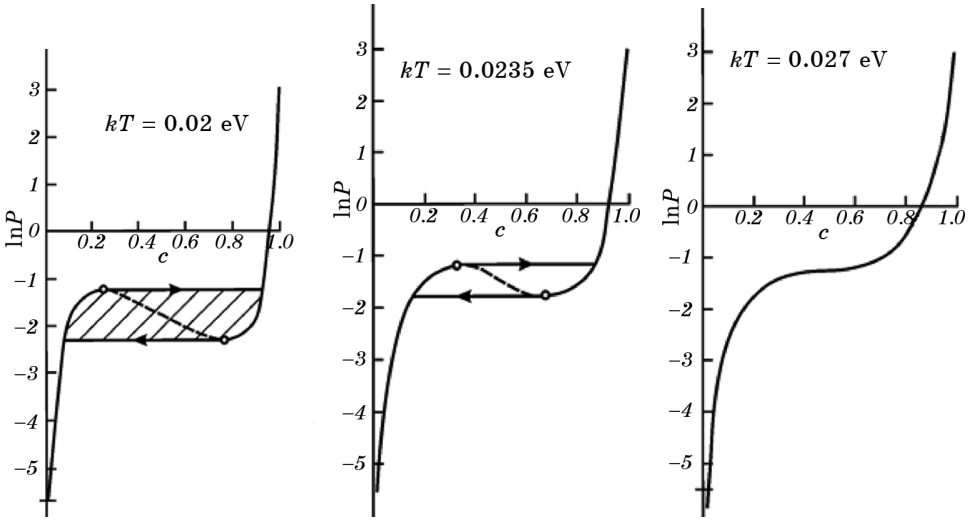

Fig. 8. Theoretical isotherms of hydrogen absorption–desorption in the zirconium–nickel metallide calculated by Eq. (18) for temperatures $kT = 0.02$, 0.235, 0.027 eV, energy parameters $u^0 = 0.37$ eV, $\alpha = -0.11$ eV, activity coefficient $D = 1\ \mathrm{MPa}^{-1/2}$, and $\beta = 0$. The extreme points are marked by circles. The regions of the curves marked by the dotted line correspond to the unstable state.

Figure 8 shows the calculated plots of the hydrogen solubility isotherms in ZrNi metallide built using Eq. (18) for different temperatures. It shows the possibility of the hysteresis effect manifestation. One can see that, with temperature increasing, hysteresis loop shortens, gets narrow and disappears. With temperature increasing, the plots pass above along axis of pressures. There is a qualitative agreement with the experimental results in Fig. 5.

The hydrogen solubility isopleths determine the dependence of natural logarithm of the pressure on the reciprocal temperature. From formula (18), one can see that this dependence is linear. In this case, the slope (tgγ) of the line is determined by the energy term $u^0 + \alpha c + \beta P$, and the value $\ln[c/(A(1-c))]$ determines the level of the line along the ordinate axis. Using experimental isopleths, the energy parameters of the system can be estimated by tgγ.

Figure 9 shows the calculated isopleths plotted with use of the Eq. (18) for different hydrogen concentrations. For the plotted graphs, the angles of inclination possess the value

$$\begin{aligned} \gamma &= -30' \text{ at } c = 0.3, \\ \gamma &= -2^\circ \text{ at } c = 0.5, \\ \gamma &= -45^\circ \text{ at } c = 0.8. \end{aligned} \qquad (21)$$

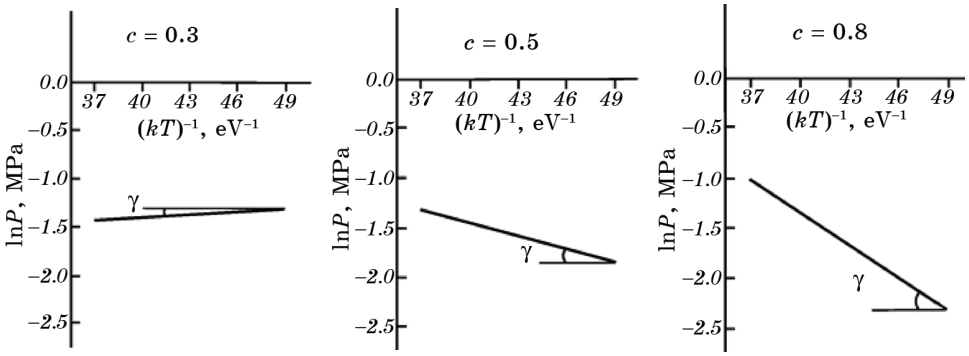

Fig. 9. Theoretical isopleths of hydrogen solubility in the ZrNi crystal calculated with Eq. (18) for hydrogen concentrations $c = 0.3$, 0.5, 0.8, energy parameters $u^0 = 0.37$ eV, $\alpha = -0.11$ eV, activity $A = 1$, and coefficient $\beta = 0$.

As seen from comparison of the calculated (Fig. 9) and experimental (Fig. 6) data, qualitative agreement is observed too. Note that a deviation of isopleths from linearity could occur with the coefficient β unequal to zero.

5. CONCLUSION

A theory of hydrogen solubility in zirconium–nickel metallide with CrB structure and with $ZrNiH_3$ trihydride forming is developed. Free energy is calculated, its temperature dependences on pressure, hydrogen content and energy parameters are determined. The equation of the equilibrium state is analysed. The hydrogen solubility dependence on the temperature and pressure is determined. It is proved that the formation of the $ZrNiH_3$ compound realizes at room temperature and atmospheric pressure. Isotherms and isopleths of hydrogen solubility are calculated. An opportunity of hysteresis effect manifestation is ascertained. With temperature increasing, the hysteresis loop shortens, gets narrow and disappears. It is found that isopleths are strictly linear. The results of calculation are compared with experimental data.

Developed theory could make it possible to choose the CrB structure material (with energy parameters known from independent experiments) for reliability accumulation and storage of hydrogen in the optimum conditions.

REFERENCES

1. R. C. Bowman, Jr., R. H. Steinmeyer, L. K. Matson, A. Attalla, and B. D. Craft, *Fusion Technol.*, **8**, No. 2: 2337 (1985).

2. S. Yang, F. Aubertin, P. Rehbein, and U. Gonser, *Zeitschrift für Kristallographie—Crystalline Materials*, **195**, Nos. 3–4: 281 (1991).
3. I. E. Nemirovskaya, A. N. Grechenko, A. M. Alekseev, and V. V. Lunin, *J. Struct. Chem.*, **32**, No. 5: 680 (1991).
4. E. Parthé, *Nekotorye Glavy Strukturnoy Neorganicheskoy Khimii (Elements of Inorganic Structural Chemistry)* (Eds. A. V. Arakcheeva and D. Yu. Pushcharovsky) (Moscow: Mir: 1993) (Russian translation).
5. S. Orimo, H. Fujii, and T. Yoshino, *J. Alloys Compd.*, **217**, No. 2: 287 (1995).
6. K. Watanabe, M. Hara, M. Matsuyama, I. Kanesaka, and T. Kabutomori, *Fusion Technol.*, **28**, No. 3: 1437 (1995).
7. L. K. Varga, K. Tompa, A. Lovas, J. M. Joubert, and A. Percheron-Guengan, *Int. J. Hydrogen Energy*, **21**, Nos. 11–12: 927 (1996).
8. V. N. Verbetsky and E. A. Movlaev, *J. Alloys Compd.*, **253–254**, No. 1: 38 (1997).
9. M. Gupta, *J. Alloys Compd.*, **293–295**: 190 (1999).
10. B. R. Simonovic, S. Mentus, R. Dimitrijevic, and M. V. Susic, *Int. J. Hydrogen Energy*, **24**, No. 5: 449 (1999).
11. N. L. Adolphi, S. Badola, L. A. Browder, and R. C. Bowman, Jr., *Phys. Rev. B*, **65**, No. 2: 024301 (2001).
12. P. Millet and P. Dantzer, *J. Alloys Compd.*, **330–332**: 476 (2002).
13. Y. D. Tasueva, P. A. Chernavskiy, N. N. Kuznetsova, and V. V. Lunin, *Vestnik Moskovskogo Universiteta. Ser. Khimiya*, **44**, No. 6: 376 (2003) (in Russian).
14. M. Prina, R. C. Bowman, and J. G. Kulleck, *J. Alloys Compd.*, **373**, Nos. 1–2: 104 (2004).
15. C. D. Browning, T. M. Ivancic, R. C. Bowman, and M. S. Conradi, *Phys. Rev. B*, **73**, No. 13: 134113 (2006).
16. I. S. Sukhushina, *Zh. Fizicheskoy Khimii*, **81**, No. 10: 1791 (2007) (in Russian).
17. D. Escobar, *Investigation of ZrNi, $ZrMn_2$, and $Zn(BH_4)_2$ Metal/Complex Hydrides for Hydrogen Storage* (Thesis ... for the Degree of Doctor of Philosophy) (Tampa, USA: University of South Florida: 2007).
18. F. Vasut, I. Stefanescu, A. Bornea, M. Zamfirache, I. Piciorea, N. Sofalca, and C. David, *Proc. of 20-th Int. Conf. 'Nuclear Energy for New Europe' (September 12–15, 2011, Bovec, Slovenia)*, p. 606.
19. X.-L. Yuan, M.-A. Xue, W. Chen, T.-Q. An, and Y. Chen, *Computational Materials Science*, **65**: 127 (2012).
20. J. Huot, D. B. Ravnsbæk, J. Zhang, F. Cuevas, M. Latroche, and T. R. Jenseb, *Prog. Mater. Sci.*, **58**: 30 (2013).
21. S. K. Dolukhanyan, *Alternative Energy and Ecology*, **31**, No. 11: 13 (2005) (in Russian).
22. A. G. Aleksanyan, A. G. Akopyan, S. K. Dolukhanyan, N. L. Mnatsakanyan, and K. A. Abramyan, *Book of Abstracts of ICHMS'2007 Conference (September 22–28, 2007, Sudak, Ukraine)*, p. 280 (in Russian).
23. G. G. Libowits, H. F. Hayes, and T. R. P. Gibb, Jr., *J. Phys. Chem.*, **62**, No. 1: 76 (1958).
24. L. N. Padurets, A. A. Chertkov, and V. I. Mikheeva, *Zh. Neorgan. Khimii*, **22**, No. 12: 3213 (1977) (in Russian).
25. L. N. Padurets, A. A. Chertkov, and V. I. Mikheeva, *Izv. AN SSSR. Neorgan. Materialy*, **14**, No. 9: 1624 (1978) (in Russian).
26. M. E. Cost, L. N. Padurets, A. A. Chertkov, V. I. Mikheeva, and E. I. Sokolova,

Zh. Neorgan. Khimii, **25**, No. 3: 847 (1980) (in Russian).
27. S. N. Endrzheevskaya, M. M. Antonova, V. V. Skorokhod, A. G. Shabalina, I. M. Shalya, and T. I. Bratanich, *Sov. Powder Metall. Met. Cer.*, **21**, No. 11: 862 (1982).
28. A. G. Aleksanyan, N. N. Agadzhanyan, A. G. Akopyan, S. K. Dolukhanyan, V. Sh. Shekhtman, H. S. Arutyunyan, K. A. Abramyan, V. S. Ayrapetyan, O. P. Ter-Galstyan, and N. L. Mnatsakanyan, *Khim. Zh. Armenii*, **55**, Nos. 1–2: 4 (2002) (in Russian).
29. A. G. Aleksanyan, H. G. Hakobyan, S. K. Dolukhanyan, N. L. Mnatsakanyan, and K. A. Abrahamyan, *Proceedings of NATO ARW 'Carbon Nanomaterials in Clean Energy Hydrogen Systems' (September 22–28, 2007)* (Dordrecht, Netherlands: Springer: 2008), p. 693.
30. A. A. Smirnov, *Obobschennaya Teoriya Uporyadocheniya Splavov* (Kiev: Naukova Dumka: 1986) (in Russian).
31. A. A. Smirnov, *Teoriya Fazovykh Prevrascheniy i Razmeshcheniya Atomov v Splavakh Vnedreniya* (Kiev: Naukova Dumka: 1992) (in Russian).
32. W. L. Larsen and M. E. Kirkpatrick, *Crystallographic Studies on the Nickel–Zirconium and Nickel–Hafnium Systems* (Report U.S. Atomic Energy Comm. IS-193: 1960), p. 66.
33. W. L. Korst, *J. Phys. Chem.*, **66**, No. 2: 370 (1962).
34. M. E. Kirkpatrick, D. M. Bailey, and J. F. Smith, *Acta Cryst.*, **15**: 252 (1962).
35. S. W. Peterson, V. N. Sadana, and W. L. Korst, *J. Phys. (Paris)*, **25**: 451 (1964).
36. H. W. Newkirk, *A Literature Study of Metallic Ternary and Quaternary Hydrides* (Report for U.S. Energy Research & Development Adm. W-7405: 1975), p. 31.
37. D. G. Westlake, *J. Less-Common Metals*, **75**, No. 2: 177 (1980).
38. T. Kajitani, H. Kaneko, and M. Hirabayashi, *Local Hydrogen Vibration in Crystalline and Amorphous Zirconium–Nickel Hydrides* (Science Reports of the Research Institutes, Tohoku Univ.: 1980), Ser. A, vol. **29**, p. 210.
39. S. N. Endrzheevskaya, M. M. Antonova ,V. V. Skorokhod, V. S. Luk'yanchikov, A. G. Shablina, I. M. Shalya, and T. I. Bratanich, *Poroshkovaya Metallurgiya*, No. 11: 39 (1982) (in Russian).
40. D. G. Westlake, H. Shaked, P. R. Mason, B. R. McCart, M. H. Mueller, T. Matsumoto, and M. Amano, *J. Less-Common Met.*, **88**, No. 1: 17 (1982).
41. I. Jacob and J. M. Bloch, *Solid State Commun.*, **42**, No. 8: 541 (1982).
42. V. A. Yartys', V. V. Burnasheva, and K. N. Semenenko, *Uspekhi Khimii*, **LII**, No. 4: 529 (1983) (in Russian).
43. S. K. Dolukhanyan, *J. Alloys Compd.*, **10–12**: 253 (1997).
44. T. Kabutomori, Y. Wakisaka, K. Tsuchiya, and H. Kawamura, *J. Nucl. Mater.*, **258–263**, No. 1: 481 (1998).
45. C. S. Moura, A. T. Motta, N. Q. Lam, and L. Amaral, *Nuclear Instruments and Methods in Physics Research B*, **180**: 257 (2001).
46. C. S. Moura, A. T. Motta, N. Q. Lam, and L. Amaral, *Phys. Res. B*, **175–177**: 526 (2001).
47. N. Michel, S. Poulat, P. Millet, P. Dantzer, L. Priester, and M. Gupta, *J. Alloys Compd.*, **330–332**: 280 (2002).
48. R. C. Bowman, N. L. Adolphi, S.-J. Hwang, T. J. Udovic, Q. Huang, and H. Wu, *Phys. Rev. B*, **74**, No. 18: 184109 (2006).

49. H. Wu, W. Zhou, T. J. Udovic, J. J. Rush, and T. Yildirim, *Phys. Rev. B*, **75**, No. 6: 064105 (2007).
50. A. Roustila, J. Chene, and C. Severac, *Int. J. Hydrogen Energy*, **32**, No. 18: 5026 (2007).
51. H. Okamoto, *J. Phase Equilibr.*, **28**, No. 4: 409 (2007).
52. M. M. Armbruster, *Reactionen von Wasserstoff mit Zintl-Phasen* (Abhandlung Dokt. der Wissenschaften) (Zürich: Techn. Universität München: 2008).
53. S. F. Matar, *Chem. Phys. Lett.*, **473**, Nos. 1–3: 61 (2009).
54. Y. Bouhadda, A. Rabehi, Y. Boudouma, N. Fenineche, S. Drablia, and H. Meradji, *Int. J. Hydrogen Energy*, **34**, No. 11: 4997 (2009).
55. X. J. Liu, X. D. Hui, G. L. Chen, and T. Liu, *Phys. Lett. A*, **373**, No. 29: 2488 (2009).
56. S. F. Matar, *Prog. Solid State Chem.*, **38**, Nos. 1–4: 1 (2010).
57. Y. Bouhadda, Y. Boudouma, and N. E. Fenineche, *Proc. of EFEEA'10 Int. Symp. on Environment Friendly Energies in Electrical Applications (November 2–4, 2010, Ghardaia, Algeria)*, p. 1.
58. Yu. L. Yaropolov, *Structure and Magnetic Properties of Hydrides of Intermetallic Compounds on the Basis of RT and R6T1, 67Si3 (R—REM; T—Ni, Co, Cu)* (Thesis ... for the Degree of Doctor of Philosophy) (Moscow: M. V. Lomonosov Moscow State Univ.: 2011) (in Russian).
59. Yu. L. Yaropolov, S. S. Agafonov, V. P. Glazkov, V. A. Somenkov, and V. N. Verbetsky, *Inorganic Materials*, **47**, No. 3: 245 (2011).
60. Yu. L. Yaropolov, V. N. Verbetsky, V. A. Somenkov, and V. P. Glazkov, *Int. J. Hydrogen Energy*, **36**, No. 3: 1222 (2011).
61. M. V. Susic, *Int. J. Hydrogen Energy*, **13**, No. 3: 173 (1988).
62. I. E. Nemirovskaya, A. M. Alekseev, and V. V. Lunin, *J. Alloys Compd.*, **177**, No. 1: 1 (1991).
63. M. E. Patt, D. M. Brennan I.T., Sacolick B.E., White U. Thomanschefsky, and E.J. Cotts, *Proc. of 7-th Int. Conf., 'Phonon Scattering in Condensed Matter' (August 3–7, 1992, New York, USA)*, No. 112, p. 528.
64. R. Kronski and T. Schober, *J. Alloys Compd.*, **205**, Nos. 1–2: 175 (1994).
65. I. E. Nemirovskaya and V. V. Lunin, *J. Alloys Compd.*, **209**, Nos. 1–2: 93 (1994).
66. N. Michel, S. Poulat, L. Priester, and P. Dantzer, *Mater. Sci. Eng. A*, **384**, Nos. 1–2: 224 (2004).
67. K. Suzuki, H. Fujimori, and K. Hashimoto, *Amorphnye Metally (Amorphous Metals)* (Ed. T. Masumoto) (Moscow: Metallurgiya: 1987) (Russian translation).
68. W. Luo, A. Craft, T. Kuji, H. S. Chung, and T. B. Flanagan, *J. Less-Common Met.*, **162**, No. 2: 251 (1990).
69. J. S. Cantrell, R. C. Bowman, Jr., L. A. Wade, S. Luo, J. D. Clewley, and T. B. Flanagan, *J. Alloys Compd.*, **231**, Nos. 1–2: 518 (1995).
70. V. Felicia, A. Preda, S. Ioan, and D. Claudia, *Asian J. Chem.*, **22**, No. 6: 4291 (2010).
71. K. J. Gross, K. R. Carrington, S. Barcelo, A. Karkamkar, J. Purewal, S. Ma, H.-C. Zhou, P. Dantzer, K. Ott, T. Burrell, T. Semeslberger, Y. Pivak, B. Dam, and D. Chandra, *Recommended Best Practices for the Characterization of Storage Properties of Hydrogen Storage Materials* (Report on the National Renewable Contract No.147388: Feb. 21, 2012), p. 579.
72. J. Nei, *Multi-Component Metal Hydride Alloys for Nickel Metal Hydride*

Battery Applications (Thesis ... for the Degree of Doctor of Philosophy) (Detroit: Wayne State Univ.: 2012).
73. Z. A. Matysina and D. V. Schur, *Vodorod i Tverdofaznye Prevrashcheniya v Metallakh, Splavakh, Fulleritakh* (Dnepropetrovsk: Nauka i Obrazovanie: 2002) (in Russian).
74. Z. A. Matysina, S. Yu. Zaginaichenko, and D. V. Schur, *Rastvorimost' Primesey v Metallakh, Splavakh, Intermetallidakh, Fulleritakh* (Dnepropetrovsk: Nauka i Obrazovanie: 2006) (in Russian).